ADAMA SCIENCE AND TECHNOLOGY UNIVERSITY

SCHOOL OF APPLIED NATURAL SCIENCE

APPLIED CHEMISTRY PROGRAM

RESEARCH PROJECT ON:

PHOTORESPONSE OF LIGNOCELLULOSE MODIFIED TiO_2 TOWARDS WATER SPLITTING FOR HYDROGEN ENERGY PRODUCTION FROM COTTON STALK DRY BIOMASS

BY

Mr. YILKAL DESSIE (PI)

Mr. SOLOMON GIRMAY

Dr. ABEBE BELAY

July, 2017

ADAMA, ETHIOPIA

ACKNOWLEDGMENTS

We would like to acknowledge our institution, Adama Science and Technology University (ASTU) for funding.

We would like to thank Addis Ababa University, Chemistry Department, and Adama Science and Technology University, Material Engineering Department for sample preparation and their characterization.

We would like to thank Dr. SENTHILKUMAR SUBRAMANIAN for his help to characterize the sample in India.

Our appreciation is also extended to the Applied Chemistry Program laboratory and research assistance for their help, support and kindness.

ABSTRACT

Photoelectron catalytic water splitting process is a promising means to solve both fossil fuel depletion and environmental pollution problems as well as for sustainable hydrogen production using renewable natural resources like sunlight and biomass. Hence, in this study the opportunity for structural development of lignocellulose (LGO) modified TiO_2 nanomaterial towards highly efficient and realistic photo-catalysis applications are evidently abundant after improved light absorption, charge-carrier dynamics, and improved particle size porosity that benefits photo-catalysis functionalities. LGO-TiO_2 nanoparticle (≈19.57 nm) for photo-catalysis was prepared via sol-gel method. The structural and morphological characterizations of the synthesized nanomaterial are carried out using UV-Vis, FTIR, XRD, SEM, and EDX techniques, based upon which the mechanistic insights are discussed. SEM analysis suggests that an average size of particle grain size is found to be in the range of 0.5-4 μm. The prepared lignocellulose modified TiO_2 satisfies the accepted energy band gap (E_g = 2.81 eV) for better photo-catalytic water splitting reaction. The photocurrent densities of regular TiO_2 and LGO-TiO_2 towards water splitting reaction under light illumination from xenon lamp were compared and found in reasonable agreement. The work also studied the application of visible light illuminated LGO-TiO_2 photo-anode photo-catalyst to the overall water splitting with a photo-conversion efficiency of 18.91% higher than that of pure TiO_2 nanoparticles. The photo-catalytic activity was extended to evaluate the decomposition of methylene blue (MB) as a testing model reaction under visible light irradiation. Therefore, parametric conditions like pH, initial concentration, and catalyst loading were examined to prove the degradation efficiency.

Keywords: *Biomass, Water-Splitting, Lignocellulose, Photo-catalyst, Methylene Blue*

TABLE OF CONTENTS

LIST OF FIGURES

LIST OF TABLES

ABBREVIATIONS AND ACRONYMS

EDX	Energy dispersive X-ray spectroscopy
FT-IR	Fourier Transform Infrared
LGO	Lignocellulose
MB	Methylene Blue
PEC	Photoelectrochemical cell
SCE	Saturated Calomel Electrode
SEM	Scanning Electron Microscope
UV-Vis	Ultraviolet and Visible spectroscopy
XRD	X-Ray Diffraction

1. INTRODUCTION

The continual increase in world population and lifestyle standards has led to a seminal growth in global energy consumption. Fossil fuel based sources of energy, such as coal, oil, and natural gas, have been used to meet the world's energy demands for a centuries. Due to this severe increasing energy demand of the modern society and limited supply of current fossil fuels, grasping alternative renewable energy sources has become one urgent and central mission for scientists. Moreover, the combustion of these fossil fuels produces large quantities of nitrogen, sulfur and carbon containing oxide pollution gases annually, which cause severe health problems for humans and global climate change. Finding renewable, clean and pollution free alternative energy sources is thus urgently needed [1].

Global focus is currently directed towards lignocellulose plant biomass valorization which not only is limited to liquid biofuel and chemicals production but also involves synthesis of reactive electrochemical intermediate. In the 21st century Lignocellulose biomass industry has become green, possible alternative of fossil resources in order to compensate the increasing trend of world's demand for petroleum usage in the chemical world. This type of biomass is the most abundantly available biopolymer in nature. It is estimated that the worldwide production of lignocellulose biomass is about 1.3×10^{10} metric tons per annum. Lignocellulose is a cross linked structure with complex carbohydrate polymer, containing polysaccharides built from sugar monomers (xylose and glucose) and aromatic polymeric material like lignin. Its chemical surface has various superior characteristics with nanoscale dimension, high surface area, unique optical properties, high crystallinity, and stiffness (comparable to Kevlar and steel) together with the biodegradability and renewability. This has made a precious green alternative material in the areas of renewable fuel production when its surface treated electrochemically with other active constituents as a photocatalyst [2, 3].

Ecological concerns have resulted in a renewed interest in natural, renewable and compostable materials, and therefore issues such as materials elimination and environmental safety are becoming an important event [4, 5]. Thus to keep the universe to be safe, functionalizing new fashion design within a perspective of sustainable growth has been applied to more and more materials [6]. Among the various materials, maximum attention has been given to TiO_2 because

of its unique characteristics such as: high photo-catalytic activity, resistance to photo-corrosion, photo-stability, low cost, nontoxicity, and due to its redox capability under ultraviolet (UV) irradiation, i.e., usually the wavelength < 385 nm [7, 8]. Additionally, such characteristics extends to extensive applications in the area of photovoltaic, sensors, optics, in dye-sensitized and solar cells, for hydrogen gas evolution, self-cleaning surfaces and environmental purification applications [9, 10].

One of the most recent nanomaterials that has been attracted a great attention due to its unique properties is titanium dioxide. It is a very useful semiconducting transition metal oxide material and exhibits a versatile material that appears in three crystalline polymorphic phases: rutile, anatase and brookite. Among the three phases maximum attentions has been given to anatase crystalline polymorphic phase this is due the highest, most effective, and widely used photo-catalyst activity and availability. The oxide nanoparticles synthesized by several methods appear more and more useful, because these nanoparticles have good electrical, optical and magnetic properties that are different from their bulk counterparts. However, since titanium oxide is cheap, non-toxic has excellent material properties, suitable energetics (band edge positions) to drive both proton reduction and water oxidation, and stability in an aqueous environment and in the area of electrochemistry [11].

Development of a photocatalyst for harvesting the practically endless sources of fuel from sunlight and water may be one of the most important challenges in any of the century. Even though, semiconductor photocatalysts are expected to be the most promising solution to the global energy demand. In exploration of efficient and economical alternative energy sources, sunlight has been recognized as a promising green and sustainable next-generation energy source owing to its abundant supply and minimum negative environmental impact. In the last three decades to an engineer titania (TiO_2) is a suitable photo-catalyst material for water splitting in an electrochemical cell as well for degradation of organic contaminants [12]. Photo-catalysis is found to be an eco-friendly cheap method for removing various pollutants from gas and liquid environments and conversion of solar energy to chemical energy by splitting water (H_2 generation) and reducing CO_2 into light hydrocarbons [13, 14].

Water is the most abundant supply of hydrogen that can be used to produce hydrogen via photocatalytic water splitting. Thus, hydrogen is considered as the energy carrier of the future as

no greenhouse gas like CO_2 is emitted when hydrogen is burnt and it can be generated from source like water. Hydrogen that is formed by the solar splitting of water is clearly considered to be the cleanest energy fuel or solar fuel to meet future demand for energy, and various attempts have been made in order to develop advanced processes to produce hydrogen. Among those techniques, photoelectrochemical cell (PEC) water splitting has attracted significant attention in the past decades as a promising renewable energy source due to their low production cost and their simplicity. Since the early 1970s, Fujishima and Honda reported a single-crystalline TiO_2 semiconductor photoanode for photoelectrocatalytic decomposition of water under UV-excitation and an external bias for the first time, great efforts have been devoted to the development of photocatalytic hydrogen production technologies [15].

In photo-electrochemical cell (PEC) system, the selection and design of the photoelectrode materials are critical since the capability of the PEC cell for water splitting is largely determined by the light absorption and carrier transport of the photoelectrode. A light active semiconductor like titanium dioxide (TiO_2) has shown great potential for hydrogen generation. As a common and inexpensive semiconductor, TiO_2 nanomaterials have been extensively explored for solar energy conversion because of their excellent electron mobility, electron-transfer efficiency, abundant morphologies and favorable environmental compatibility. However, wide bandgap in TiO_2 limits the photoelectrochemical (PEC) water splitting performance due to poor absorption of visible light. Therefore, it’s urgent to search for a strategy to simultaneously increase the light capture.

2. STATEMENT OF THE PROBLEM

Fashioning UV-Visible active photocatalytic nanomaterial, renewable energy production and environmental challenges are paramount issues in the 21st century. Titanium dioxide offers a series of advantages over other semiconductor photocatalysts: high catalyst stability, low toxicity and low cost. TiO_2 has poor adsorption and photocatalytic activity towards decomposition of organic pollutants which can be considered a limitation if the concentration of pollutant is very low. In addition splitting of water in to hydrogen and oxygen using titanium oxide as a working electrode in the electrophotochemical cell system is a serious challenge.

This study is expected to give baseline information on improving the photocatalytic performance of TiO_2 using lignocellulosic materials to alter its band gap. The doped TiO_2 is an extrinsic semiconductor (electroactive nanomaterial) i.e., it has different electrical properties than an undoped or intrinsic semiconductor. Therefore, one of the previous main problems using TiO_2 nanoparticulate photocatalyst system is clearly identified from the discussion of this research based on spectral and spectroscopy facts.

3. SIGNIFICANCE OF THE STUDY

Ethiopia is highly rich in dry biomass lignocellulosic materials comprising from hard and soft wood plants. There is thus the need to seek alternative energy sources. In the country using energy directly from solar environment for different application is not much common. In addition adapting the synthesis nanotechnology would result in a unique next generation of wood based products that have hyper-performance and superior serviceability when used in severe environments including photocatalyst and producing renewable energy production like hydrogen through modification. The prepared nanomaterial in the photo-electrochemical cell system as a photoelectrode has the advantages of improved light absorption efficiency in the visible region and better charge separation. Capturing solar energy with semiconductor through modification by plant matter is the best selective, cheap, non-corrosive, and chemically stable technique.

4. OBJECTIVES

4.1. General Objective

- The main objective of this work was to study the photoresponse of lignocellulose modified TiO_2 nanomaterials towards water splitting for renewable energy production.

4.2. Specific Objectives

- To build up a visible light-sensitive photocatalyst nanomaterial from lignocellulosic biomass towards water splitting.
- To characterize the modified TiO_2 Nanostructure material using UV-Vis spectra, FTIR, scanning electron microscope (SEM), Energy dispersive X-ray spectroscopy (EDAX) and X-ray diffraction (XRD).
- To determine and visualize the degradation efficiency of lignocellulose modified TiO_2 nanomaterial by using methylene blue as a testing model followed by controlling parameters.

5. LITERATURE REVIEW

5.1. Photocatalyitic Mechanism

Solar energy reduction efficiency of environmental pollutant gases with the art of different photo-catalytic systems, including biological (plants and algae), inorganics (semiconductors), organics (molecular complexes), and hybrid (enzyme/semiconductors) systems are the recent strategy due their effective activity, selectivity and stability. Alternatively, heterogeneous catalysts are preferable in terms of stability, separation, handling, and reuses, as well as reactor design, which reflect no problems in solubility and miscibility, are the strengths of a heterogeneous system in order to reduce the cost of production. Heterogeneous catalysis has a fundamental role in the development of sustainable industrial processes, as it potentially possesses the ability to achieve the objectives of industrial catalysis, while paying attention to the principles of sustainable and green chemistry [16].

Among the various photo-catalytic materials that have been used, most attention has been focused on titanium dioxide (TiO_2) as a photo-catalyst in diverse areas ranging from water and air treatment to self-cleaning surfaces. Photodegradation is defined by the International Union of Pure and Applied Chemistry (IUPAC) as "The photochemical transformation of a molecule into lower molecular weight fragments, usually in an oxidation process". Recently, photo-catalytic activity of immobilized TiO_2 particles on macro-porous ceramic alumina foams has been reported [17].

Electrons in the outermost orbit called valence electrons are responsible for bonding and excitation when it is exposed to light of 380 nm or lower and responsible for the formation of two band gaps called conduction band (higher in energy) and valence band (lower in energy). Conduction band electrons (e^-) and valence band holes (h^+) are first generated on the surface of photo-catalyst particles when the aqueous catalyst suspension is illuminated by light with energy greater than the band gap energy, i.e., 3.2 eV. Then the adsorbed pollutant molecules onto the nanocatalysts are then oxidized by free radicals. Like hydroxyl radicals, formed by the "positive holes" in the valence band accepting electrons from hydroxyl ions, are the catalytically active intermediates formed in aqueous solution thereby resulting in the photo-catalytic effect. When titanium dioxide is irradiated with light that exceeds its band gap energy (3.2 eV for anatase) i.e.

UV light (wavelength <385 nm for anatase), electron-hole pairs are created. The electron-hole pairs degrade organic pollutants on the catalyst surface either directly or indirectly in a water solution by creating hydroxyl and superoxide radicals. Sometimes direct charge-transfer causes the oxidation. However, discussion of light absorption in semiconductor photo-catalysis is generally restricted to extending absorption to longer wavelengths (to harvest a greater proportion of solar radiation) and the possibility of photo-sensitizing reactions by exploiting electron transfer to the semiconductor from excited states of adsorbed dyes [18].

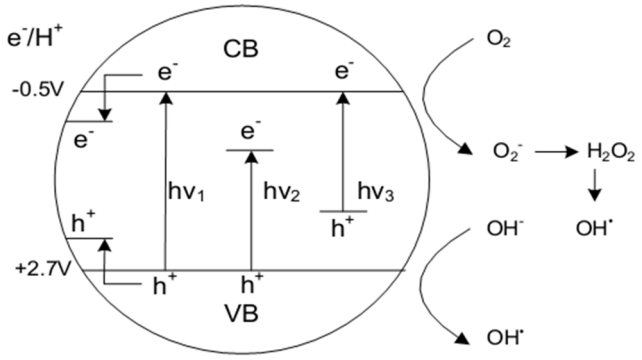

Figure 1: Schematic mechanism of doped TiO_2 photocatalysis. $h\nu_1$: pure TiO_2; $h\nu_2$: metal-doped TiO_2 and $h\nu_3$: nonmetal-doped TiO_2.

5.2. Method to Synthesis Nanomaterial's

There have been significant approaches to fabricate various nanocatalysts, including high-voltage acceleration technique, sol-gel method, coprecipitation-peptization, and template-assisted synthesis [18]. Up to now, the improvement of the photo-catalytic reactivity still search for further investigations. One way to improve the photo-catalytic capability is to increase available active areas for photo-degradation of pollutant molecules in vapor or liquid-phase. Indeed, the selection of a suitable support as host material is necessary for the above purpose. There are several porous media, such as zeolite, carbon nanotube, aerogel, and active carbon, which as far as possible provide pore structures for dispersing TiO_2 photo-catalysts [19]. Apart from the supports mentioned above, lignocellulose is an emerging material due to its multi-functionality including a regular and parallel porosity infrastructure, i.e., lengthwise and crosswise.

5.3. Lignocellulose Biomass

Biomass is the term used to describe all the organic matter produced by photosynthesis that exists on the earth's surface and is available in varying quantities throughout the developing world [20]. It is categorized into three distinct parts such as Solid biomass, Biogas, and Liquid Biofuels. Burning biomass is not the only way to release its energy. Transition metals modified with hard wood biomass can be converted to other usable forms of renewable energy through modification like methane gas or transportation fuels like ethanol and biodiesel. The dry matter biomass, so called lignocellulose biomass is the most abundantly available raw material for the production of bio-fuels like bio-ethanol. It is composed of carbohydrate polymers (cellulose, hemicellulose), and an aromatic polymer (lignin) [4, 21].

Photocatalytic reforming may be a promising alternative as mild reaction conditions driven by solar light (i.e., room temperature and atmospheric pressure) can be comparatively advantageous to such energy-consuming thermochemical processes. Hydrogen production by photocatalytic reforming of lignocellulosic biomass may also be more feasible and practical as compared to photocatalytic water splitting due to its potentially higher efficiency. The thermodynamics of photochemical water splitting were reported to store a maximum of only 12% of the incident light energy [22].

The photocatalytic water splitting processes is initiated when a nanomaterial photo catalyst absorbs photons with energies greater than its band gap energy (Eg). Therefore, any semiconductor photocatalyst should possess band gap energy (Eg) greater than 1.23 eV to be used for water splitting. In order to be excited by the visible light irradiation its value should be less than the catalyzed energy 3.0 eV, i.e. for photo catalyzed materials for visible light water splitting which satisfy these two requirements of proper band gap energy (1.23 eV< Eg <3.0 eV) and band positions [23].

Lignocellulosic biomass-derived compounds can also serve as sacrificial agents (electron donors) to reduce the photo-catalyst recombination e^{-}-h^{+} rate. A large variety of organic compounds (most of them model compounds of lignocellulose structure, e.g. alcohols, polyols, sugars, as well as organic acids) have been used as electron donors for photocatalytic hydrogen production [24].

Lignocellulosic materials such as wheat straw, bagasse, pine, peanut, cotton straw and poplar sawdust have attracted a lot of attention recently. Many studies have investigated the effects of different novel biomass-derived fillers on the synthesis and properties of different metal oxide nanostructures. Gelatin, gum, starch, rice straw, tunicates and cotton were all investigated to synthesize metal oxide nanoparticles such as ZnO, TiO_2, and Ag nanoparticles [25]. Therefore, in this study, we investigate the effects of extracted cotton stalk powder on properties of calcined TiO_2 nanoparticles via sol-gel method.

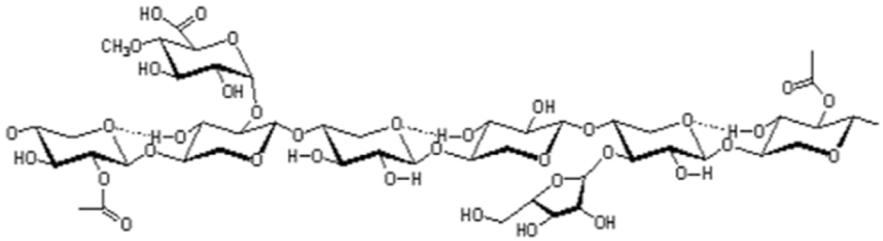

Figure 2: Hemicellulose backbone [26].

In the lignocellulose complex ether bond, ester bonds, carbon-to-carbon bonds, and hydrogen bonds are the most common types of bonds. These bonds are common in both intra-polymer and inter-polymer linkages.

Table 1: Cross-link structure in lignocellulose biomass

Bonds	**Intra-polymer linkages**	**Inter-polymer linkages**
Ether bond	Lignin, hemicellulose	Cellulose-Lignin Hemicellulose-Lignin
Carbon to carbon bond	Lignin	
Hydrogen bond	Cellulose	Cellulose-Hemicellulose
Ester bond	Hemicellulose	Hemicellulose-Lignin

6. MATERIALS AND METHODS

6.1. Chemicals and Reagents

Titanium oxide (titania), ethanol, methanol, acetone, sodium hydroxide, sulfuric acid, and distilled water. All chemicals and reagents used in this study were analytical grade. Commercial amorphous anatase titanium dioxide (titania: TiO_2) and azo-dye (methylene blue, $C_{16}H_{18}ClN_3S$) were used as a base material and as a model organic compound for photo-catalytic test.

6.2. Apparatus and Instruments

Scanning electron microscope (SEM), X-ray diffraction (SHIMADZU, XRD-7000 X-RAY DIFFRACTOMETER), UV-Vis spectrophotometer, and fourier transform infrared spectrum 65 FT-IR (Bruker IFS120 M, PerkinElmer), aluminium foil, oven, beaker, volumetric flask, conical flask, heat mantle, rounded bottom flask, condenser, mortar, crusher, mass balance, funnel, graduated cylinder, glove, and polyethylene bag.

6.3. Pretreatment and Extraction

Raw cotton stalk dry biomass was chopped and reduced into smaller pieces followed by washing with cold distilled water.

6.3.1. Soxhlet Extraction

Dried raw biomass, 35 g, was loaded into the cellulose thimble in Soxhlet extractor set up, and 1000 mL of acetone was used as solvent for extraction. The boiling temperature was carefully adjusted to 45^{o}C and 25 min respectively on the heating mantle for a 4 hour run period. After extraction, the sample was air dried at room temperature and 1.5 g of extracted dried biomass was transferred into a 250 mL Erlenmeyer flask then150 mL of 500 mol/m^3 NaOH was added. The mixture was boiled for 3.5 hour with distilled water. It was filtered after cooling through vacuum filtration and washed until neutral pH. The residue was dried and~6% wt was collected [27].

6.3.2. Water and Alkali Extraction

20 g air dry material was extracted with water at 80^{o}C for 1 hour using a dry biomass ratio of 1:10. The mixture was vacuum filtered in a Buchner funnel and then washed with 500 ml water.

The water extracted material was further extracted with 20 wt% sodium hydroxide (NaOH) solution at 80^{o}C for 1 hour to dissolve the lignin and to obtain lignocellulose. After the mixture was filtered the alkali extract was collected, and the residue was washed with water until the pH was neutral [28]. Finally, the extract was dried and around 38% wt yield was collected.

6.4. Photocatalyst Preparation

Commercial available anatase titanium dioxide shows an acidic reaction. So, the investigated material was washed with ammonia solution to neutralize the acidic solution. The solution was washed with distilled water to remove the excess ammonia and the final pH was recorded as (7.17-7.19). Subsequently, TiO_2 was dried at 80 ^{o}C for a few hours and grounded with a mortar then after it was kept ready for further analysis [29].

Lignocellulose (LGO) modified TiO_2 material was synthesized as follows: 6 g of amorphous TiO_2 and 5 g of LGO were mixed with 25 mL of distilled water for 6 hours at 90 ^{o}C using water bath and then air-cooled at room temperature. The resulting product was collected and washed thoroughly with distilled water, and finally dried at 60 ^{o}C in an oven. The obtained powders (pH = 6.94- 6.97) were dried for 24 hours at the temperature of 80 ^{o}C and calcinated in a muffle furnace at 400 ^{o}C for 2 hours [30].

6.5. Characterization of Lignocellulose Modified TiO_2 Nanomaterials

Lignocellulose (LGO) modified TiO_2 nano materials and photo-oxidation of methylene blue under UV and Visible light were used to characterize and evaluate the photo-catalytic activity of the obtained samples over a range of 200-800 nm. Fourier transform infrared Spectrum 65 FT-IR (Bruker IFS120 M, PerkinElmer) were recorded in the range 4000-400 cm^{-1} using KBr pellets under standard conditions. The crystal structure of the powders was analyzed using Scanning Electron Microscopy (ZEISS EVO 18), Energy Dispersive X-ray Spectroscopy (EDAX) with INCA software for quantitative analysis and XRD (SHIMADZU, XRD-7000 X-RAY DIFFRACTOMETER), and the XRD patterns were collected in 2θ range from 10 to 80 in degrees with a Cu target and an x-ray tube at 40 kV and 30 mA.

6.6. Photoelectrochemical characterization

Photoelectrochemical cell (PEC) was operated on an electrochemical workstation (CHI 660E, CH instruments) using three electrode system with a photoanode as a working electrode, coiled Pt wire as a counter electrode and Hg/Hg_2Cl_2 as a reference electrode, and 0.5 M Na_2SO_4 (with pH buffered at 6.75) purged with N_2, solution was applied as a supporting electrolyte. The working electrode was fabricated by securing a copper wire on the exposed electric conductive part of fluorine-doped tin oxide (FTO) with transparent glass paint. TiO_2 and LGO-TiO_2 nanoparticles were used as a photoanode (working electrode, with an area of 3 cm^2). The water splitting photoelectrode was illuminated at100 mW/cm^2 with a power density from 150W xenon lamp with in the entire solar spectrum.

6.7. Degradation Methylene Blue

The photocalytic degradation of MB by LGO-TiO_2 photocatalysts were performed under visible light irradiation. The photocalytic degradation was monitored using UV-Vis light irradiation at $\lambda_{max} = 420\, nm$ as a light source using 250 Watt xenon lamp. In all experiments a 160 mg of catalyst was suspended in 100 mL of 6 ppm methylene blue solution in a conical flask. The flask was wrapped with aluminium foil then placed in the dark for an hour for adsorption to take place. The system was then irradiated with visible light from a lamp that was fixed in the middle of the system and 12 cm above the surface of the solution. To detect changes in concentration, aliquots of methylene blue solution (5 mL) were taken after every 30 minutes and centrifuged followed by measuring the absorbance of the clean solution by UV-Vis spectrometer [31]. The concentration of MB was proportional to its absorbance according to Beer-Lambert law, so the degradation efficiency of organic compound (MB) was calculated using the following formula [32]:

$$\text{Degradation efficiency} = \frac{C_o - C}{C_o} \times 100\% = \frac{A_o - A}{A_o} \times 100\% \quad \ldots\ldots (1)$$

Where C_o and C concentration before and after degradation while A_o and A absorbance before and after degradation, respectively.

6.8. Statistical Analysis

The drawing curves of the data obtained were performed using Origin 8 software and Microsoft Excel.

7. RESULTS AND DISCUSSIONS

7.1. UV-Vis Spectra of LGO Modified TiO_2 Nanoparticles

The UV-Vis absorbance spectra of TiO_2, LGO and LGO-TiO_2 are illustrated in figure 3(A) and compared with the absorbance of unmodified TiO_2 nanoparticles LGO modified TiO_2 nanoparticles have a light harvest performance between 400nm-500nm (λ_{max} ~442 nm). Compared to the unmodified nanomaterial's the modified TiO_2 using LGO from dried cotton stalk display a better shift of absorption edge towards the visible region. According to the report given from table 2 and increases in wave length as well as red shift from the curve indicated due to titanium-ester new bond formation (fast electron transfer from p- orbitals of carbon to d-orbitals of Titanium) and an effective surface modification after alkaline pretreatment [33]. Sodium hydroxide causes the disruption of hydrogen bonding in cellulose and hemicellulose, breakage of ester linkages between lignin and deprotonation of phenolic groups. As a result, swelling of cellulose and the partial solubilization of hemicellulose and lignin occurs from the lignocellulose polymer [34]. The band near 300 nm in the UV- visible absorption spectrum from figure 3(A) shows due to the presence of unconjugated phenolic units in the extracted lignocellulose material. Figure 3(B) shows UV- Vis absorbance spectra LGO modified TiO_2 and unmodified nanoparticles at specified maximum wavelength. According to the beer lamberts law as the concentration of the given sample raises the absorption capacity also increases.

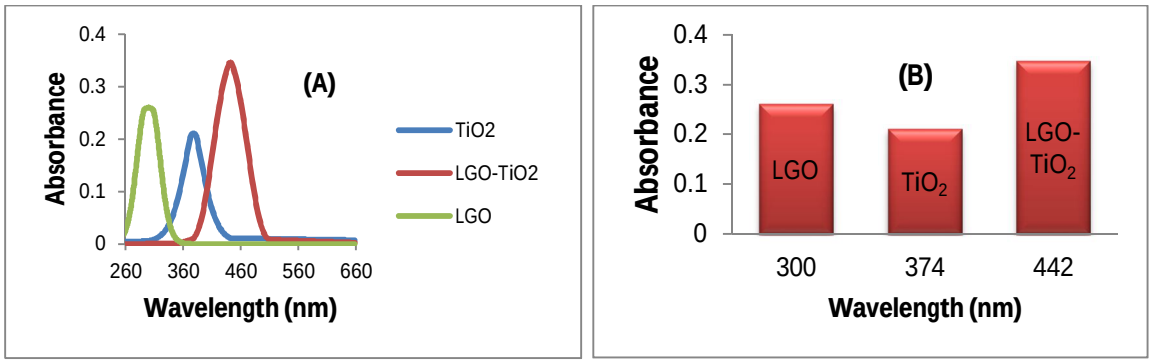

Figure 3: (A) UV-Vis absorption spectra of LGO (light green), TiO_2 (blue), and LGO-TiO_2 (red) nanoparticles, (B) Change in absorption spectra and their maximum wavelength, λ_{max} at 160 mg powder.

7.2. Photocatalytic Activity of LGO-TiO_2 Nanoparticles

In this study photocatalytic of MB was used as the model organic pollutant to evaluate the activity of LGO modified TiO_2 nanomaterials. Figure 4(a) shows the UV-Vis diffuse reflectance spectra of methylene blue solution before and after visible light irradiation ($\lambda = 420\,nm$) for different contact time (minutes). The characterstic absorption bands of this organic pollutant solution at (λ_{max}~$664\,nm$) were significantly decreased in intensity with increasing irradiation time. The absorbance of this peak approaches to a minimum value and the removal (degradation) efficiency shown from figure 4(b) become effective after illumination for 150 minute.

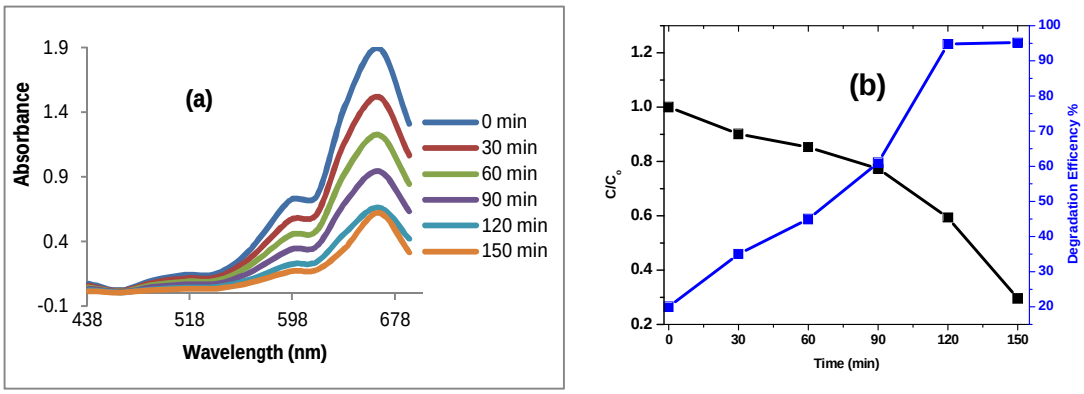

Figure 4: (a) Absorption spectral changes and photodegradation of Methylene Blue (b) degradation efficiency on titania loaded LGO under visible light irradiation ($\boldsymbol{\lambda > 420\,nm}$). Reaction conditions: C_o = 6 ppm, catalyst loading: 160 mg, pH = 6, T = 27±2^oC

7.3. Photodegradation Process and Energy Band Gap

In the presence of air or oxygen, the activated semiconductor nanoparticles are capable of decomposing many organic contaminants [16]. The activation of LGO-TiO_2 by light (hv) produces electron-hole pairs which are powerful oxidizing and reducing agents, respectively.

$$LGO - TiO_2 + hv \rightarrow h^+ + e^- \quad \text{.....(2)}$$

The oxidative and reductive reactions are:

$$OH^- + h^+ \rightarrow {\cdot}OH \quad \text{and} \quad O_2 + e^- \rightarrow O_2^- \quad \text{.....(3)}$$

In the degradation of organic compounds like methylene blue (MB), the hydroxyl radical which comes from the oxidation of adsorbed water or adsorbed OH^- is the primary oxidant and the presence of oxygen or electron reach site can prevent the re-combination of hole-electron pairs [18].

$$MB + {}^{\cdot}OH \rightarrow CO_2 + H_2O + NH_4^+ + NO_3^- + SO_4^{2-} + Cl^- \quad \ldots\ldots(4)$$

A visible-light photocatalyst activity with a small band gap is important. Criterion for the degradation of organic compound is the redox potential of $H_2O/{}^{\cdot}OH$ ($OH^- \rightleftharpoons {}^{\cdot}OH + e^-$; $E^o = -2.8$ V) couple lies within the band gap of the semiconductor [18]. The difference and smaller band gap of LGO-TiO_2 gives active response to the visible light as shown in table 2 and Figure 5 below.

Table 2: Maximum wavelength and energy band gap for TiO_2, LGO, and LGO-TiO_2

	Experimental Value		**Reported Value**		
Nanocrystals	(λ_{max})	$E_g = \frac{hC}{\lambda_{max}}$	(λ_{max})	$E_g = \frac{hC}{\lambda_{max}}$	[35]
LGO	300 nm	4.14 eV	290 nm	4.28 eV	[36]
TiO_2	378 nm	3.28 eV	387 nm	3.2 eV,	[11, 37]
LGO-TiO_2	442 nm	2.81 eV			

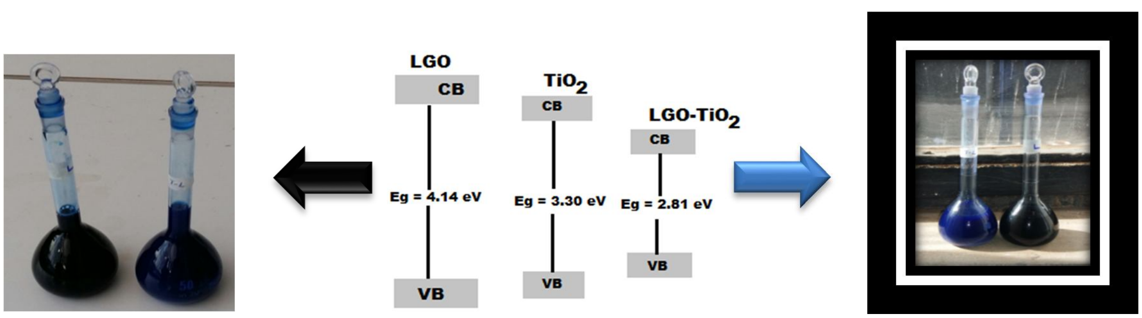

Figure 5: MB degradation in the absence of light before degradation (left time = 0 min), Schematic band structure (middle) and MB degradation after degradation (right, time = 150 min).

7.4. FT-IR of LGO-TiO_2 Nanoparticles

FT-IR spectroscopy was used to analyze the prepared photocatalyst in the range of 4000-400 cm^{-1}. Thus, from Figure 6 and Figure 7 showed that the FTIR spectrum of bulk and LGO modified TiO_2 nanoparticls. The peaks at around 2922 $cm^{-1}$and 2850 cm^{-1} shows C-H asymmetric and symmetric vibration mode of CH_2 groups, respectively. The peaks around at 630 cm^{-1} assigned to the characterstics vibration of Ti-O-Ti network in the titanium dioxide [11]. The broad peak at 3433 cm^{-1} corresponds to the stretching vibration of hydroxyl groups in the lignocellulosic material. The broad peak observed at about 490 cm^{-1} found in Ti-O is due to out of plane bending [11] and in the range observed from 950-1100 cm^{-1} corresponds to the interaction between the Ti-O network and the C=O in the hemicellulose polymer. More intense peak at around 1100-1150 cm^{-1} is the characteristics of C-O stretching due to the presence of ether or ester bond in the lignocellulose polymer [38].

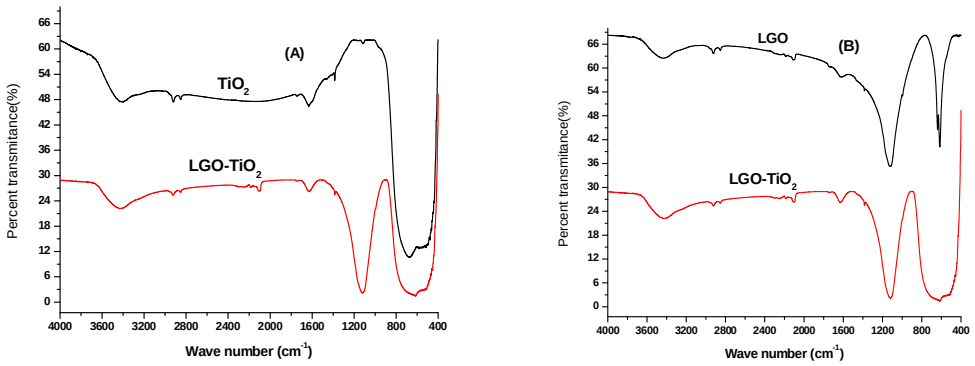

Figure 6: (A) FT-IR spectrum of TiO_2 (black) and LG-TiO_2 (red) and (B) LGO (black) and LG-TiO_2 (red).

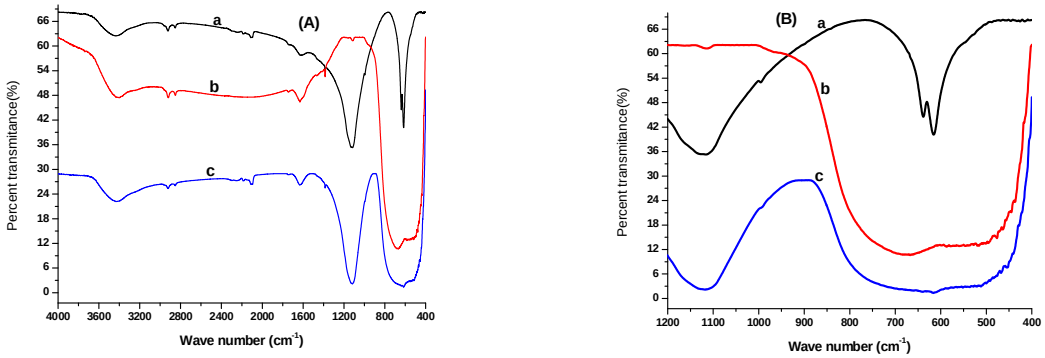

Figure 7: (A) FT-IR spectrum of LGO (a) black), (b) TiO_2 (red) and (c) LG-TiO_2 (blue) and (B) the stretching FT-IR spectrum in the range 1200-400 cm^{-1}.

7.5. Powder XRD Analysis

The XRD spectrum of LGO, TiO_2, and LGO-TiO_2 nanoparticles are shown in Figure 8. The consecutive and being peaks in lignocellulose doped TiO_2 shows the characteristic appearance of the modified material treated at 400^oC for 2 hours. The major diffraction peaks at 2θ values are 19.06, 25.32 and 32.14. The crystallite size can be calculated from the classical Debye-Scherrer equation, $D = K\lambda/\beta\cos\theta$, where, D is the crystallite size, λ= 0.1541 nm, is the wavelength of the X-ray CuKα radiation, K is Scherrer constant (usually taken as 0.9 for spherical like nanoparticles), β is the Bragg's diffraction angle or full-width half-maximum (FWHM) value. Therefore, from Table 3 the average crystallite size of lignocellulose modified TiO_2 nanomaterial is in the range between 17-20 nm [11]. In addition the observed peaks are sharp indicates the prepared sample was pure.

Table 3: Average nano-crystallite sizes for TiO_2, LGO and LGO-TiO_2.

Nano-crystals	β (FWHM)/degree	D (Crystallite size)/nm
TiO_2	0.16000	19.81
LGO	0.16010	21.44
LGO-TiO_2	0.14915	19.57

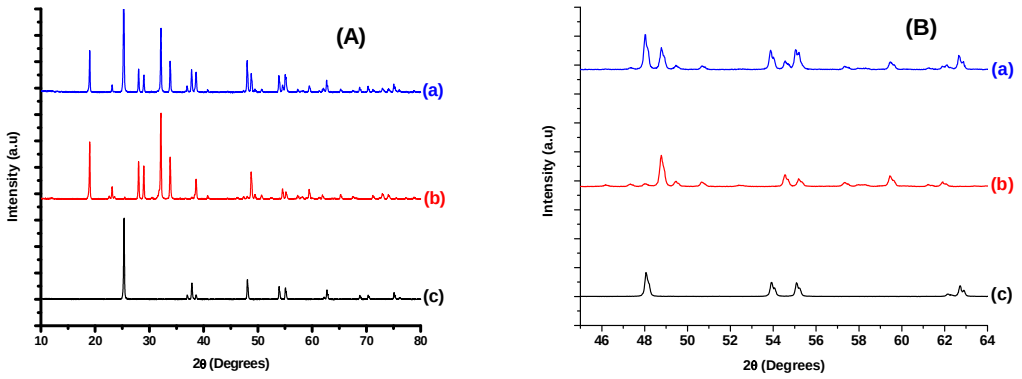

Figure 8: (A) XRD patterns of (a) LGO-TiO_2 (blue), (b) LGO (red) and (c) TiO_2 (black) nanoparticles and (B) XRD pattern in the range between 44-64 (2θ Degree).

7.6. Scanning Electron Microscopy (SEM) and (EDAX)

Measurements from SEM provide information about the surface topography on the prepared crystal surface of the sample. In Figure 9 (B) crystals has a very small size which investigated from XRD results and LGO is clearly and well spread across the crystal surface of TiO_2 after 400^oC calcination. This could be caused by the presence of solvent trapped in the crystal structure of TiO_2 could be explained from the emergence of carbonyl functional group after previously obtained from FTIR spectra. The morphology of titania powders calcined at the same temperature in Figure 9 (A) exhibited irregular morphology due to the agglomeration of main particles. In all cases the average size is found to be nearly spherical and its grain size is going to be in the range of 0.5-4 μm. From the images a homogeneous type of coating and the adhesive interaction between inter-particle interactions was clearly observed over wide areas that shown from Figure 9(B).

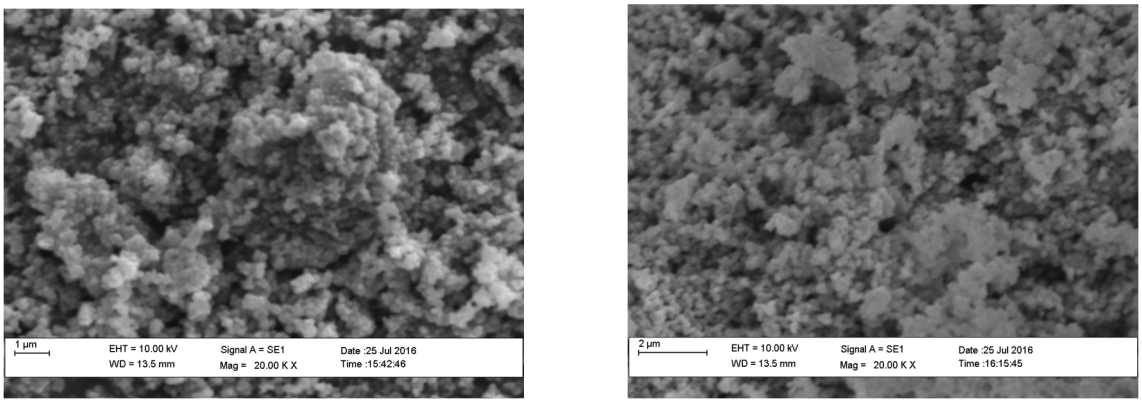

(A) **(B)**

Figure 9: (A) SEM images of 6 wt% LGO modified TiO_2 and (B) 50 wt% LGO modified TiO_2 calcined at 400^oC.

The surface elemental compositions of the as prepared photoanodes were further identified by Energy Dispersive X-ray Spectroscopy (EDAX) measurement, and the atomic ratios were calculated from the EDX spectrum. The result shown in Figure 10 (A) and (B) SEM image investigations followed by chemical compositions peaks (atomic and weight %, table 4) with elements; titanium (Ti), oxygen and carbon could be clearly seen in the survey and it clearly showed no trace of any other impurities could be seen within the detection limit of the spectrum.

Table 4: Elemental composition (atomic %) of 6 wt% LGO and 50 wt% LGO doped nanomaterial films, treated at 400^{o}C.

	6 wt% LGO-TiO_2			**50 wt% LGO-TiO_2**			**Total**
	Elements			Elements			
	Ti	O	C	Ti	O	C	
Atomic %	25.31	59.52	15.17	18.91	50.50	30.59	100
Weight %	51.65	40.58	7.77	43.52	38.82	17.66	

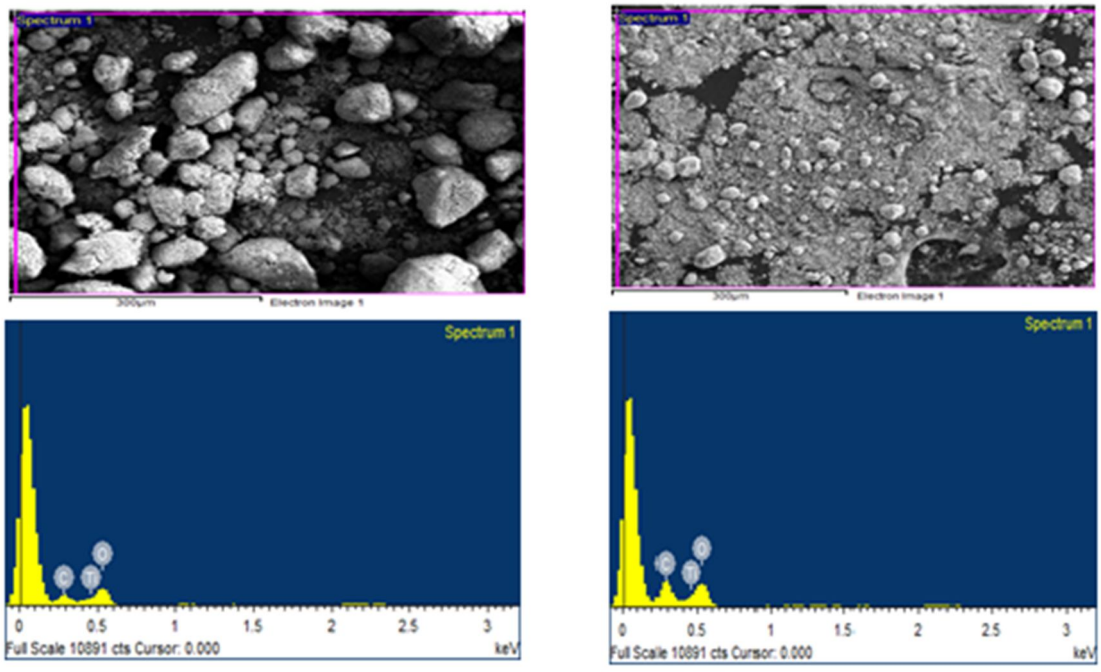

(A) **(B)**

Figure 10: (A) SEM micrographs coupled EDAX spectrum result of 6 wt% and (B) 50 wt% LGO-doped TiO_2 nanoparticles.

7.7. Photocatalytic Water Splitting Efficiency

7.7.1. Photocurrent Density on Measured Electrode Potential

Plots of Photocurrent density (j_p, Acm^{-2}) as a function of measured potential, E_{meas} (V/SCE) for TiO_2 and LGO-TiO_2 calcined at 400^oC were shown in Figure 11(A). Curve (a), i.e., unmodified TiO_2 shows the lower photocurrent density of 9.95 mA cm^{-2} with respective potential at -0.88 V/SCE. The observed low photocurrent density was due to low surface functionality and slow electron transfer across its crystalline structure while Curve (b), i.e., LGO-TiO_2 displayed the higher photocurrent density when it compared with bare TiO_2 sample and its maximum photocurrent density value, 16.51 $mAcm^{-2}$ was recorded at a potential of -0.76 V/SCE with in the same environment. This indicates that LGO-TiO_2 is a good photo-response nano-conducting material for the transfer and deterioration of the photo-induced electrons. The surface modification of TiO_2 using LGO was successful and increased the effective surface area of an oxide layer causes generation in higher photocurrent density, i.e., fast electron transfer could exist across the whole surface of the functionalized nanomaterial. Such increment allows the material could absorb more light to generate more electron-hole pairs (excitation) for the targeted application.

7.7.2. Dependence of Photoconversion Eficiency on Applied Potential

The corresponding visible spectrum efficiencies from figure 11(B) were found to be 11.24% and 18.91% for TiO_2 and LGO-TiO_2, respectively, under illumination intensity of 100 mW cm^{-2} from a 150 watt Xenon lamp. The increase in anodic film photocurrent efficiency near to the electrode surface corresponds to an increase in grain size particle to volume ratio that results higher PEC water splitting efficiency. Therefore, the overall schematic degradation efficiency shown from figure 11(C) and calculation of total percent photoconversion efficiency (%ε_{photo} (total)) of light energy was carried out using the equation [39].

$$\%\,\varepsilon_{photo}\,(\text{total}) = \frac{j_p[E^o_{rev} - |E_{app}|]}{P_o} \times 100 \quad \text{.....(5)}$$

where j_p is the photocurrent density (mW cm^{-2}), E^o_{rev} is the standard reversible potential (which is 1.23 V for water splitting reaction), P_o is the power density of incident light (mW cm^{-2}), $|E_{app}|$ is the absolute value of the applied potential.

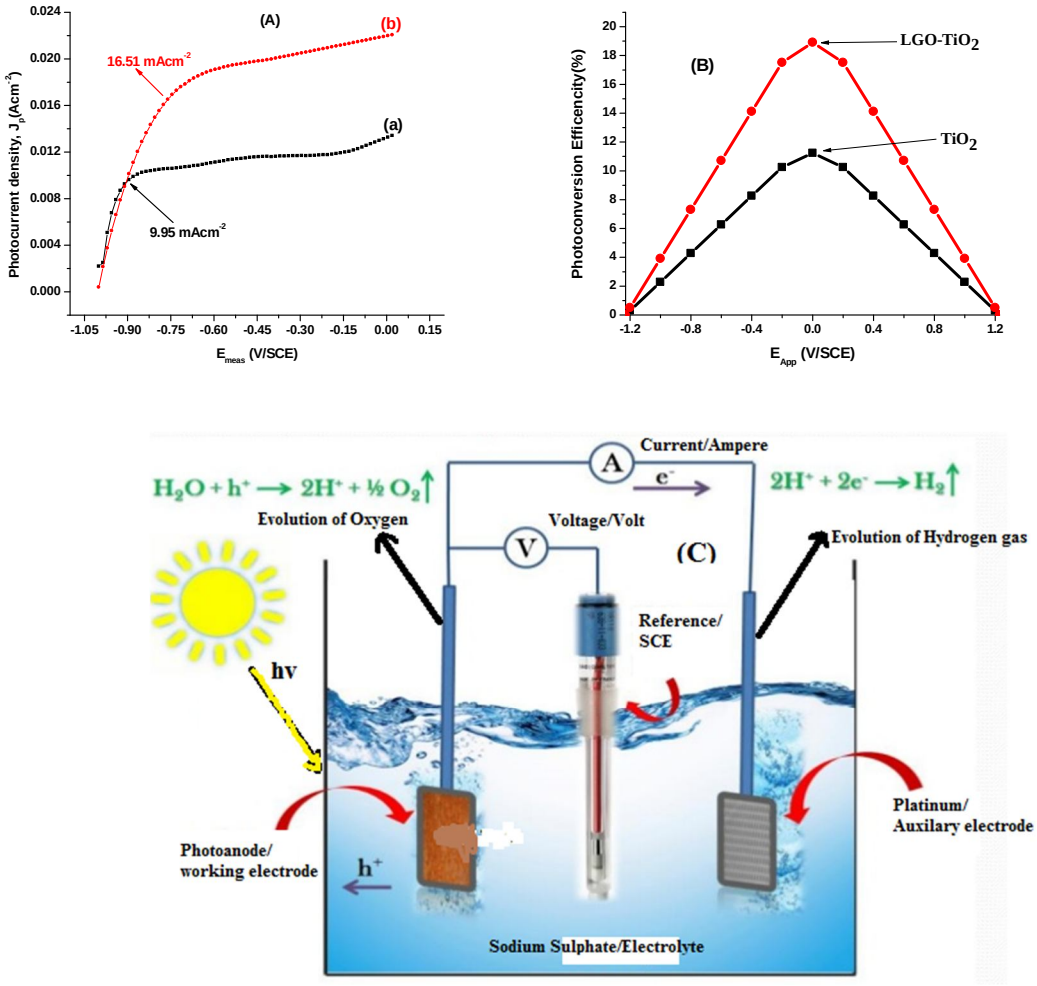

Figure 11: (A) Photocurrent density, j_p as a function of measured potential, E_{meas} (V/SCE), (B) Dependence of photoconversion efficiency, % ε_{photo} (total), on applied potential E_{app} (V) for TiO_2 (black) and LGO-TiO_2 (red) and (C) Schematic representation of three electrode systems.

7.8. Parameter Optimization

7.8.1. Effect of pH solution

The role of pH on the efficiency of photocatalytic degradation of MB was carried out in the range of 3-9; the results are plotted in Figure 12. At pH (3-5.5), molecules of MB are adsorbed on photocatalyst surface due to the undessociation nature of MB thereby producing higher photocatalytic efficiency (95 %, at pH = 6), then decrease in efficiency due to negatively charged nature of photocatalyst surface at higher pH (higher alkalinity). Thus, lower degradation of MB

is observed in the alkaline environments. Related results were reported in the unmodified TiO_2 photocatalyst with the pH value from 4 to 8 efficiency 90 % [40].

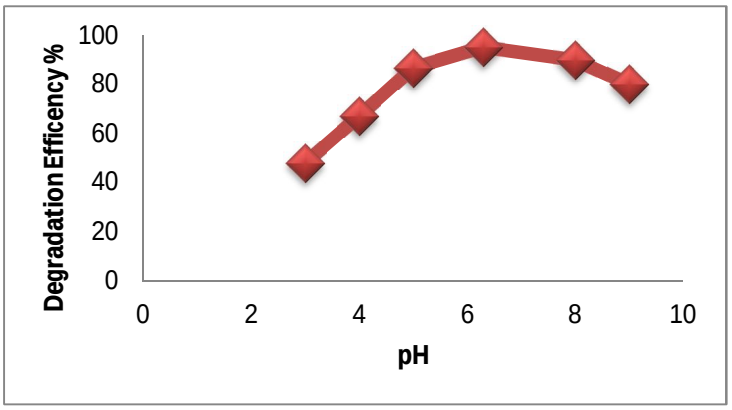

Figure 12: Effect of pH solution on degradation efficiency of methylene blue with concentration of 6 mg/L, 160 mg loading catalyst, time = 120 min, T = 27± 2^{o}C.

7.8.2. Effect of Photocatalyst Loading

Figure 13 shows effect of catalyst loading at different amount of LGO, i.e., 57.14 % LGO, 50 % LGO and 44.44 % LGO on the degradation of methylene blue in the range 140 mg to 180 mg by optimizing other conditions. The photodegradation efficiency was increased from 140 mg to 160 mg and reached at a maximum of 160 mg at around 2 hour irradiation time. Then decrease in efficiency was observed at maximum TiO_2 suspension due to increase in turbidity and low light penetration of a catalyst that is reported from earlier studies [41].

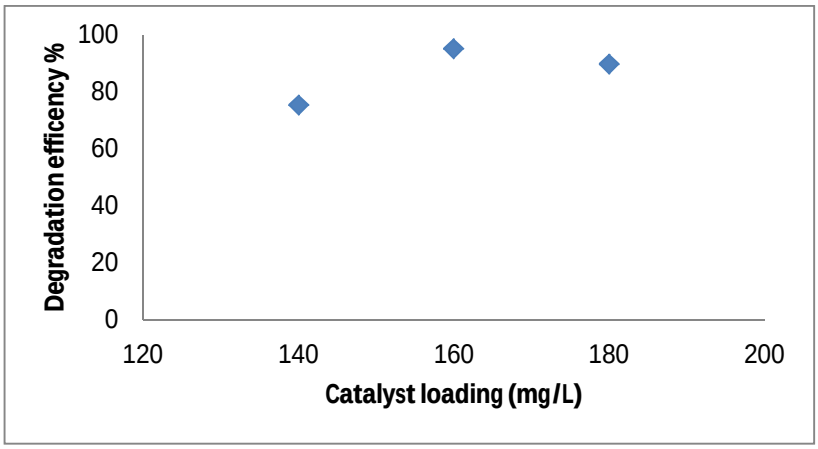

Figure 13: Effect of catalyst loading on degradation efficiency of methylene blue with concentration of 6 mg/L, pH = 6, time = 120 min, T = 27± 2^{o}C.

8. CONCLUSIONS

Solar water splitting accompanied with photocatalytic organic pollutant degradation is recognized as a potential science and technology advancement for solving fast depletion of fossil fuel and serious environmental problems. Pure TiO_2 and lignocellulose (LGO) modified photocatalysts were successfully fabricated through sol-gel method and then treated at 400^oC calcination temperature. The catalytic performances of LGO-TiO_2 sample was investigated as a good photocatalytic active nanomaterial for water splitting and methylene blue (MB) degradation. The results showed that LGO-TiO_2 nanostructures annealed at 400°C was better for MB degradation; i.e., ≈ 95 % degradation efficiency and better for PEC water splitting for hydrogen renewable solar fuel evolution; i.e., photo-conversion efficiency ≈ 18.91% than that of pure TiO_2 and this suggests that the energy band gap (UV-Vis), surface functionality (FTIR), surface topography (SEM), porosity and particle size (XRD), and purity and chemical composition (EDX) of prepared sample was successfully functionalized. Finally, parameters such as solution pH, catalyst amount and initial concentration were effectively studied. 6 pH, 160 mg catalyst load and 6 mg/L concentration were determined as optimum conditions for the experiment. Therefore, such photocatalysis was proved to be a good-looking method to remove such pollutants from its source.

9. RECOMMENDATIONS

Based on the above findings the following recommendations were made:

- Experimental building photocatalysis and theoretical mechanistic studies should possibly develop a new generation of highly stable and selective photocatalysts for oxidative organic trans-formations including those of lignocellulosic derivatives from which we hope to actively participate in future years to come.
- A cooperative effort is needed to explore potential nanomaterial as a conducting material that will generate the highest solar-to-hydrogen efficiency. The development of new technologies requires collaboration with a strong theoretical background for a better understanding of the hydrogen production mechanism in order to come up with a low-cost and environmentally friendly water-splitting process for hydrogen production.
- Studies of MB that can be photodegraded by LGO modified TiO_2 should be undertaken using sunlight as a direct illumination sources.

10.REFERENCES

[1] M. R. Gholipour, C-T. Dinh, F. Béland and T-O Do, Nanocomposite heterojunctions as sunlight-driven photocatalysts for hydrogen production from water splitting, *Nanoscale*, vol. 7, pp. 8187-8208, 2015.

[2] J.-P. Lange, I. Lewandowski, and P. M. Ayoub, "Cellulosic biofuels: a sustainable option for transportation," in Sustainable Development in the Process Industries, pp. 171-198, John Wiley & Sons, NewYork, USA, 2010.

[3] I. Siró and D. Plackett, "Microfibrillated cellulose and new nanocomposite materials: a review," Cellulose, vol.17, pp.459-494, 2010.

[4] M. M. Pavlović, V. Ćosović, M. G. Pavlović, N. Talijan and V. Bojanić, Electrical Conductivity of Lignocellulose Composites Loaded with Electrodeposited Copper Powders, International Journal of Electrochemical Science, vol. 6, pp. 3812-3829, 2011.

[5] X-J YANG, S. Wang, H-M Sun, X-B Wang and J-S Lian, Preparation and photocatalytic performance of Cu-doped TiO2 nanoparticles, Transactions of Nonferrous Metals Society of China, vol. 25, pp. 504-509, 2015.

[6] L. S. Daniel, H. Nagai, N. Yoshida and M. Sato, Photocatalytic Activity of Vis-Responsive Ag-Nanoparticles/TiO_2 Composite Thin Films Fabricated by Molecular Precursor Method (MPM), *catalysts*, vol. 3, pp. 625-645, 2013.

[7] A. Gautam, A. S. Kshirsagar, S. Banerjee, V. V. Dhapte and P. K. Khanna, UVC-Shielding by Nano-TiO_2/PMMA Composite: A Chemical Approach, *Journal of Materials Science & Nanotechnology*, Vol. 4, pp.1-14, 2016.

[8] G. Yang, Z. Jiang, H. Shi, T. Xiao and Z. Yan, Preparation of highly visible-light active N-doped TiO_2 photocatalyst, *Journal of Materials Chemistry*, vol. 20, pp. 5301-5309, 2010.

[9] M. Fekadu and S. Feleke, Biomass energy production technologies of fast pyrolysis and transesterification: a review, *International Journal of Emerging Technology and Advanced Engineering*, vol. 4, pp. 629-637, 2014.

[10] C-H Wu, J-F Shr, C-F Wu and C-T Hsieh, Synthesis and photocatalytic characterization of titania-supported bamboo charcoals by using sol–gel method, *Journal of Materials Processing Technology*, vol. 203, pp. 326-332, 2008.

[11] S. Perumal, K. MonikandaPrabu, C. G. Sambandam and A. P. Mohamed, Synthesis and Characterization Studies of Solvothermally Synthesized Undoped and Ag-Doped TiO_2 Nanoparticles Using Toluene as a Solvent, *International Journal of Engineering Research and Applications*, Vol. 4, pp.184-187, 2014.

[12] S. Bagheri, D. Ramimoghadam, A. T. Yousefi and S. B. A. Hamid, Synthesis, Characterization and Electrocatalytic Activity of Silver Doped-Titanium Dioxide Nanoparticles, *International Journal of Electrochemical Science*, vol.10, pp. 3088-3097, 2015.

[13] G. D. Scholes, G. R. Fleming, A. O. Castro and R. V. Grondelle, Lessons from nature about solar light harvesting, *Nature chemistry*, vol. 3, pp. 763-774, 2011.

[14] P. Silija, Z. Yaakob, V. Suraja, N. N. Binitha and Z. S. Akmal, An Enthusiastic Glance in to the Visible Responsive Photocatalysts for Energy Production and Pollutant Removal, with Special Emphasis on Titania, *International Journal of Photoenergy*, vol. 2012, pp. 1-20, 2011.

[15] Yongkun Li, Hongmei Yu, Wei Song, Guangfu Li, Baolian Yi, Zhigang Shao, A novel photoelectrochemical cell with self-organized TiO_2 nanotubes as photoanodes for hydrogen generation, *International Journal of Hydrogen Energy*, vol. 36, pp. 14374-14380, 2011.

[16] R. Bindig, S. Butt, I. Hartmann, M. Matthes and C. Thiel, Application of Heterogeneous Catalysis in Small-Scale Biomass Combustion Systems, *Catalysts*, vol. 2, pp. 223-243, 2012.

[17] S. Kamel, Nanotechnology and its applications in lignocellulosic composites, a mini review, *eXPRESS Polymer Letters*, vol.1, pp. 546-575, 2007.

[18] N. Soltani, E. Saion, M. Z. Hussein, M. Erfani, A. Abedini, G. Bahmanrokh, M. Navasery and P. Vaziri, Visible Light-Induced Degradation of Methylene Blue in the Presence of Photocatalytic ZnS and CdS Nanoparticles, *International Journal of Molecular Sciences*, vol. 13, pp. 12242-12258, 2012.

[19] P. Dhatshanamurthi, B. Subash, B. Krishnakumar, M. Shanthi, Highly active ZnS loaded TiO_2 photocatalyst for mineralization of phenol red sodium salt under UV-A light, *Indian Journal of Chemistry*, vol. 53A, pp. 820-823, 2014.

[20] J. R. Bolton, S. J. Strickler and J. S. Connolly, Limiting and realizable efficiencies of solar photolysis of water, *Nature*, vol. 316, pp. 495-500, 1985.

[21] R. Luque and A. M. Balu, ed, Producing Fuels and Fine Chemicals from Biomass Using Nanomaterials. Taylor and Francis Book Inc., New Jersey, 2013.

[22] Donya Ramimoghadam, Samira Bagheri, and S harifah Bee Abd Hamid, Biotemplated Synthesis of Anatase Titanium Dioxide Nanoparticles via Lignocellulosic Waste Material, Volume 2014, Article ID 205636, 7 pages.

[23] J. S. Lee, Photocatalytic water splitting under visible light with particulate semiconductor catalysts, *Catalysis Surveys from Asia*, Vol. 9, pp.217-227, 2005.

[24] D. G. Dawit, Assessment of Biomass Fuel Resource Potential and Utilization in Ethiopia: Sourcing Strategies for Renewable Energies, *International Journal of Renewable Energy Research*, Vol. 2, pp. 1-9, 2012.

[25] A. G. Temesgen and O. Sahu, Process ability enhancement of false Banana fiber for rural development, *Journal of Agricultural Economics, Extension and Rural Development*, vol. 1, pp. 064-073, 2014.

[26] Kirk-Otmer 4^{th} edition (2001).

[27] A. O. Ayeni, O. A. Adeeyo, O. M. Oresegun, T. E. Oladimeji, compositional analysis of lignocellulosic materials: Evaluation of an economically viable method suitable for woody and non-woody biomass, *American Journal of Engineering Research*, vol. 4, pp. 14-19, 2015.

[28] W. Ren, Z. Ai, F. Jia, L. Zhang, X. Fan and Z. Zou, Low temperature preparation and visible light photocatalytic activity of mesoporous carbon-doped crystalline TiO_2, *Applied Catalysis B: Environmental*, vol. 69, pp. 138-144, 2007.

[29] K. Bubacz, J. Choina, D. Dolat and A. W. Morawski, Methylene Blue and Phenol Photocatalytic Degradation on Nanoparticles of Anatase TiO_2, *Polish Journal of Environmental Studies*, vol. 19, pp. 685-691, 2010.

[30] M. Lezner, E. Grabowska and A. Zaleska, Preparation and Photocatalytic Activity Of Iron-Modified Titanium Dioxide Photoc Atalyst, *Physicochemical Problems of Mineral Processing*, vol. 48, pp. 193-200, 2012.

[31] R. Rajkumar and N. Singh, To Study the Effect of the Concentration of Carbon on Ultraviolet and Visible Light Photo Catalytic Activity and Characterization of Carbon Doped TiO_2, *Journal of Nanomedicene and Nanotechnolgy*, vol. 6, pp. 260-266, 2015.

[32] Y. Abdollahi, A. H. Abdullah, Z. Zainal and N. A. Yusof, Photocatalytic degradation of p-Cresol by zinc oxide under UV irradiation, *International Journal of Molecular Science*, vol. 13, pp. 302-315, 2011.

[33] F. Chen, W. Zou, W. Qu, Jinlong Zhang, Photocatalytic performance of a visible light TiO_2 photocatalyst prepared by a surface chemical modification process, *Catalysis Communications*, vol.10, pp. 1510-1513, 2009.

[34] H. V. Lee, S. B. A. Hamid and S. K. Zain, Conversion of Lignocellulosic Biomass to Nanocellulose: Structure and Chemical Process, *The Scientific World Journal*, Vol. 2014, 2014, Article ID 631013, 20 pages.

[35] Jeremy Wade, An Investigation of TiO_2-$ZnFe_2O_4$ Nanocomposites for Visible Light Photo catalysis, A thesis submitted to Department of Electrical Engineering; College of Engineering, University of South Florida, March 24, 2005.

[36] C. A. Lekelefac, N. Busse, M. H. errenbauer and P. Czermak, Photocatalytic Based Degradation Processes of Lignin Derivatives, *International Journal of Photoenergy*, Vol. 2015, 2014, Article ID 137634, 18 pages.

[37] M. M. Ba-Abbad, A. A. H. Kadhum, A. B. Mohamad, M. S. Takriff and K. Sopian, Synthesis and Catalytic Activity of TiO_2 Nanoparticles for Photochemical Oxidation of Concentrated Chlorophenols under Direct Solar Radiation, *International Journal of Electrochemical Science*, vol. 7, pp. 4871- 4888, 2012.

[38] A. A. Guilherme, P. V. F. Dantas, E. S. Santos, F. A. N. Fernandes and G. R. Macedo, Evaluation Of Composition, Characterization And Enzymatic Hydrolysis of Pretreated Sugar Cane Bagasse, *Brazilian Journal of Chemical Engineering*, Vol. 32, pp. 23 - 33, 2015.

[39] S. U. M. Khan, M. Al-Shahry, W. B. Ingler Jr, Efficent Photochemical water splitting by a chemically Modified n- TiO_2, *Science*, Vol. 297, pp. 2243-2245, 2002.

[40] Dr. Salmin S. Al-Shamali, Photocatalytic Degradation of Methylene Blue in the Presence of TiO_2 Catalyst Assisted Solar Radiation, *Australian Journal of Basic and Applied Sciences*, Vol.7, pp. 172-176, 2013.

[41] M. N. Chong, B. Jin, C. W. K. Chow, C. Saint, Recent developments in photocatalytic water treatment technology: A review, *Water Research*, Vol. 44, pp. 2997-3027, 2010.